Int J Thermophys (2010) 31:1027–1036
DOI 10.1007/s10765-010-0734-8

Water Transport Monitoring in Calcium Carbonate Stones by Photoacoustic Spectroscopy

J. May-Crespo · P. Martínez-Torres · J. J. Alvarado-Gil · P. Quintana · J. Ordóñez-Miranda

Received: 19 June 2009 / Accepted: 30 March 2010 / Published online: 13 April 2010

Abstract Calcium carbonate is the most abundant inorganic material, and it was used to build the ancient Mayan monuments in the peninsula of Yucatán, México. One of the most important challenges that these structures have to confront is related to water and its transport inside the stone that induces serious deterioration. In this study, the photoacoustic (PA) technique is used to monitor the water permeability of two kinds of solid and compacted powdered stones. The analysis of water permeability in stones is performed using a modified Rosencwaig PA cell. When the stones are in contact with the water reservoir, the PA signal amplitude is observed to decay gradually due to the progressive wetting of the sample. Based on this type of experiment, the water diffusion coefficients as well as the time evolution of the thermal effusivity are obtained.

Keywords Calcium carbonate stones · Photoacoustic spectroscopy · Water diffusion · X-ray diffraction

1 Introduction

The study of movement of fluids through stones has been the subject in several fields of research and technology such as engineering on ground water, petroleum, and geology and also in soil physics, building materials, from which numerous applications have been derived such as contaminant transport, storage of nuclear waste, hydrocarbon

J. May-Crespo (✉) · P. Martínez-Torres · J. J. Alvarado-Gil · P. Quintana · J. Ordóñez-Miranda
Applied Physics Department, Cinvestav-Unidad Mérida, Carretera Antigua a Progreso, Km. 6, Col. Gonzalo Guerrero, CP 97310, Mérida, Yucatán, México
e-mail: jmayc@mda.cinvestav.mx

J. J. Alvarado-Gil
e-mail: jjag09@yahoo.com

recovery, stone durability, biodeterioration, etc. [1–7]. The transport of water in building construction stones and historical monuments is one of the most important factors determining their durability, as it favors weathering processes such as acid dissolution in calcareous materials, growth of biological species, crystallization of soluble salts, and the swelling-contraction cycles due to hydration and temperature changes during day and night, in tropical environments [2,8,9].

It is well known that the transport properties of rocks are conditioned by their permeability and porosity systems, since they control the movement and storage of fluids in stones. These properties represent important characteristics of materials that would allow an understanding of the influence of water on engineering construction, such as water leakages to evaluate affluent to a foundation pit or as indicators for the utilization of various kinds of rocks for building construction [10]. Sandstones are mainly used for various purposes in the building industry, for the renovation of historical buildings, stonework, etc. Limestone and arenaceous marl are used as facing materials for restoration of historical buildings; marlite is used for building foundations, etc. Permeability is one of the rock properties that have a strong impact on rock weathering and is necessary for solving hydrological and hydrogeological problems [8,10,11].

The Yucatan peninsula is a flat plain with very low elevations above sea level consisting of calcareous sediments of the Cenozoic. The calcareous rock of the Yucatan peninsula has a very heterogeneous distribution of physical and mechanical properties, due to various diagenetic environments involved in their formation, which are typical of sedimentary calcareous rocks of shallow tropical seas with an abundance of reef and coralline structures [12]. The most resistant and durable calcareous rocks have been used by the Mayan culture population to construct their monumental buildings and roads that have lasted over time without important subsidence and deformation. Actually, they are used for cement and lime manufacture; they are also utilized as crushed stone aggregates for concrete and road basis, and on a small scale, as building stones for columns, walls, facades, etc.

Several techniques, like fluorescence microscopy, confocal laser scanning microscopy, nuclear magnetic resonance, etc., have been applied to study, at the microstructural level, water diffusion in different classes of porous materials, including paper [13], powders, rocks, and soils [12]. These techniques involve complicated methodologies; and it is therefore desirable to have simple reliable techniques. During recent years the photoacoustic (PA) spectroscopy technique has been demonstrated to be a useful tool in materials characterization and in the study of diffusion and evaporation processes of a liquid in porous media [14–16]. The versatility of these techniques is based on the fact that they look directly at the heat generated in a sample, due to non-radiative de-excitation processes, following the absorption of the modulated light that impinges upon the sample [17].

Recently, there has been great interest to study the dynamic evolution of different systems using photothermal (PT) techniques [18–21]. One of the most useful procedures in the study of dynamical systems consists of the measurement of the PT signal during the time evolution of the physical system, maintaining a fixed modulation frequency of the light source. The PT signal is not only directly related to the time evolution of the thermal properties, but also with different physical processes leading to modulated heat, and additionally with changes in the geometry of the sample [17].

PA techniques have been used to monitor in real time, the evolution of different processes, such as oxygen release during the photosynthesis process and oxygen evolution in plants [18,22], gas adsorption and desorption in porous substances [23,24], real-time monitoring of the gas concentration in a binary gas mixture [25], detection of adulterants in automotive fuels [26], evaporation dynamics [27], effects of changes in geometry on the PA signal when a solvent is evaporated inside of a ring [28,29], etc.

In this study, the potential of the PA technique in monitoring in real time, the water transport in stones of calcium carbonate of the peninsula of Yucatan in Mexico is explored. It is shown that the PA signal shows a systematic change when the process evolves. Using an effective model, it is demonstrated that the water transport can be understood in terms of the time evolution of the material thermal properties.

2 Materials and Methods

2.1 Sample Preparation and Characterization

The stones S and T were collected from different sites of the north of Yucatan, Mexico. The studied rocks belonged to two different lithological groups: S, crystallized or consolidated limestone (called *laja*) that is a hard layer located underneath the soil at 0.3 m to 2.5 m, and T, a soft rock, coquina limestone, designated regionally as *sahcab*, and is located deeper at 2.5 m to 5 m [12]. The samples for measurements were polished with sandpaper until a smooth flat surface was obtained, followed by cleaning with ultrasonication in ethanol. The final thickness of the samples was 1 mm, and their diameters were 6 mm.

The second set of samples was from the same type of stone (SP and TP); they were ground in an agata mortar until a fine powder (<2 μm) was obtained. These samples (0.1 g) were compacted into pellets (7 mm diameter) with about 1 Ton pressure and named SP and TP. In both cases at the end of the polishing or grinding process, the samples were dried in a furnace at 110 °C for 4 h.

Scanning electron microscopy (SEM) and chemical analysis by energy dispersive X-ray spectroscopy (EDXS) were performed in an environmental scanning electron microscope Philips model XL30, which has an EDXS attached. Structural characterization was carried out by X-ray diffraction (XRD) in a Siemens D-5000 diffractometer operated at 35 kV and 25 mA, with Cu Kα radiation ($\lambda = 1.5418$ Å). The rocks samples were placed in a glass sample holder and registered within 3° to 45° 2θ range, with a time step of 6 s and a step size of 0.02°. Calcium carbonate was dissolved with a 5 % HCl solution in order to see the presence of other minerals, and registered by XRD.

2.2 PA Technique

The permeability of the rock samples was analyzed by the PA technique. It consists of a conventional PA cell (Fig. 1a), closed on one side by a transparent window and on the other by aluminum foil of 25 μm thickness [30]. On top of this foil, the sample stone was attached using thermal paste. An electret microphone is used, coupled to the

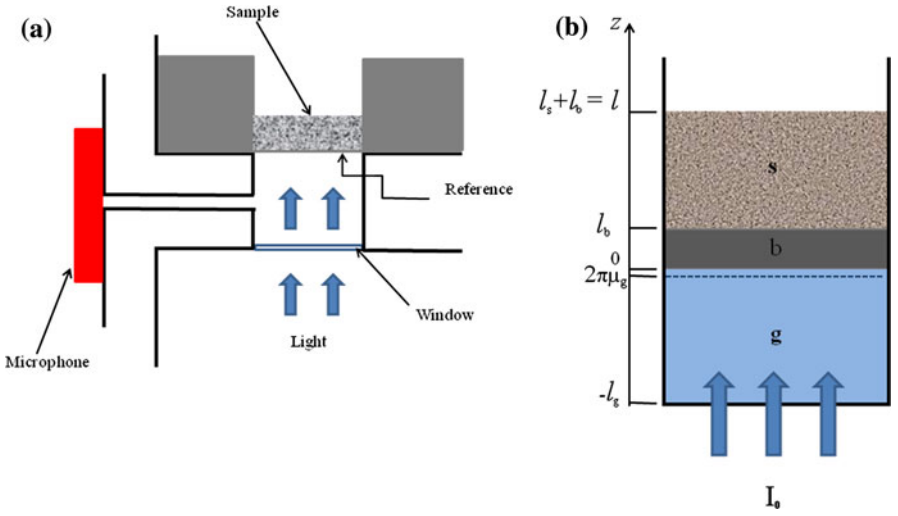

Fig. 1 (**a**) Schematic cross section of the conventional PA cell and (**b**) Configuration of the PA cell

cavity wall, to register the pressure fluctuations in the PA chamber produced by the periodic heating of the aluminum, due to the pumping beam of a 160 mW diode laser at 658 nm (ML120G21) modulated at a constant frequency ($f = 7$ Hz). The microphone signal is fed into a lock-in amplifier (SR830), from where the output signal amplitude is recorded, as a function of time, in a personal computer.

During the PA experiment, using a micropipette, a water drop of 50 μL was deposited on top of the sample. As a result of the water permeation process, the PA signal shows a systematic decay during the subsequent stages. In order to get results independent of the specific characteristics of the microphone, the PA signal at any time was normalized dividing by the PA signal before the water drop was deposited.

The physical configuration of these experiments is schematically represented in Fig. 1b. A modulated laser beam, $I(t) = I_0(1+\cos(\omega t))/2$ with $\omega = 2\pi f$, is impinging into the internal surface of the substrate (b), of thickness l_b, which is in contact with air (g) of the chamber. For these experiments the stone (s), of thickness l_s, is the sample to be studied. According to Rosencwaig and Gersho theory [31], the PA signal is determined by temperature fluctuation θ, at the air–substrate interface ($Z = 0$). Solving the thermal diffusion problem for the configuration shown in Fig. 1b and considering that the main role of the aluminum substrate is a light-heat converter, it is found that the spatial part of the modulated temperature is

$$\theta = \frac{I_0}{2k\sigma}\left[\frac{(\mathrm{g}+1)\mathrm{e}^{\sigma l} - (\mathrm{g}-1)\mathrm{e}^{-\sigma l}}{(\mathrm{g}+1)^2\mathrm{e}^{\sigma l} - (\mathrm{g}-1)^2\mathrm{e}^{-\sigma l}}\right], \tag{1}$$

where $\sigma = (1+\mathrm{i})a$ is the complex thermal diffusion coefficient of the sample, with a defined by $(\pi f/\alpha)^{1/2}$, $\mathrm{g} = \varepsilon_\mathrm{g}/\varepsilon$ is the thermal coupling coefficient, where ε_g is the thermal effusivity of air and ε is that of the sample. For the modulation frequencies

used in this study, considering that the samples are very thick, the thermal diffusion length of the sample is much smaller than the sample thickness ($\mu = a^{-1} \ll l$). Based on this, and taking into account that the thermal effusivity of air is much smaller than that for the sample, Eq. 1 can be written as

$$\theta = \frac{I_0}{2\sqrt{\pi f}(1+\mathrm{i})\varepsilon}. \tag{2}$$

In this approximation, the PA signal only depends on the inverse of the thermal effusivity of the sample and the modulation frequency. When the modulation frequency is fixed, for thermally thick samples, the normalized temperature would only depend on the thermal interchange of the sample with the surroundings. Changes in the temperature would be due to the time evolution of the thermal effusivity.

3 Results and Discussion

The analyzed samples, consolidated limestone S and coquina limestone T, were observed by optical microscopy (Fig. 2a and b) and showed the following differences: the former has a smooth surface with patches of calcite with a different hue coated with a very fine-grained carbonated cement, and in some areas it was possible to detect the presence of small pores; the latter sample shows a rough surface with a homogeneous grain composition, although it has a large number of voids and a porous space structure. From SEM images (Fig. 2c and d) the consolidated limestone showed an amorphous shape with pores with sizes 2 μm to 100 μm, which was detected inside of the pores well-formed calcite crystals; for the coquina limestone microporous of 5 μm to 10 μm and a heterogeneous distribution of amorphous calcite was observed. From EDS analysis no strong differences in composition were detected; for sample S the composition was 44.78 % Ca, 16.61 % C, and 38.6 % O, and for sample T, the composition was 43.89 % Ca, 17.36 % C, and 38.75 % O.

The XRD patterns of the raw material (Fig. 3) show a majority phase calcite ($CaCO_3$) for both samples SP and TP. However, after carbonate dissolution, the diffractograms show the presence of small quantities of quartz, hematite, and clays (chamosite and kaolinite) for SP, and smectite, kaolinite, and quartz for TP. The coquine stone shows a higher proportion of calcite than the consolidated rock.

The PA signal amplitude behavior as a function of time for S and T limestones is shown in Fig. 4a for both samples. The first stage (0 to 200 s) is related to the PA signal before the drop water is placed on top of the sample. For the consolidated limestone S, the PA signal shows a second stage in which a rapid decay from 200 s up to 800 s occurs, due to wetting of the stone, and a third stage becomes stationary for $t > 800$ s. On the other hand, for the coquina limestone, T, the time interval of the second stage is smaller occurring from 200 s up to 450 s, and afterward, the signal is constant, similarly to the behavior of the S stone.

The decay of the signal as a function of time for both samples can be interpreted as a process of water transport in the stone. However, as can be observed, the transport process in T is faster than in S (Fig. 4a).

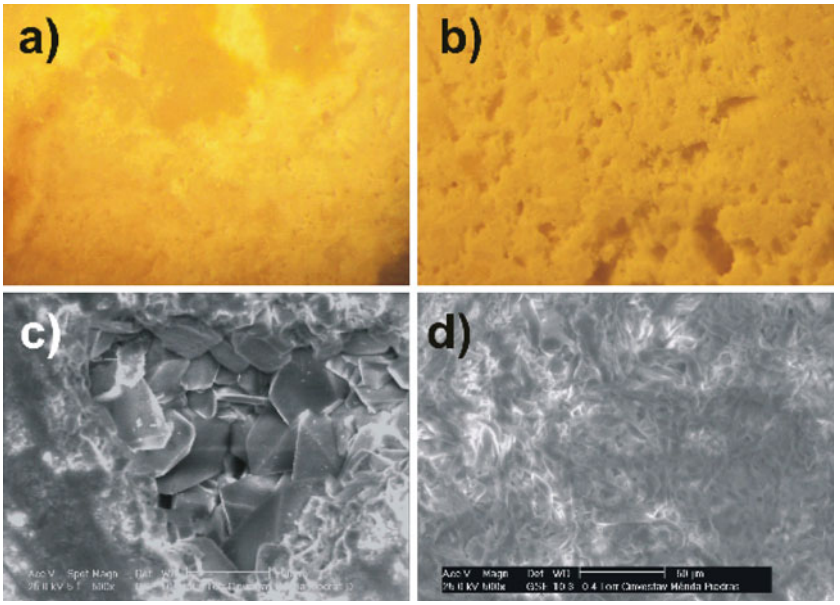

Fig. 2 Optical microscope images and SEM micrographs for the limestones: (**a**, **c**) S and (**b**, **d**) T

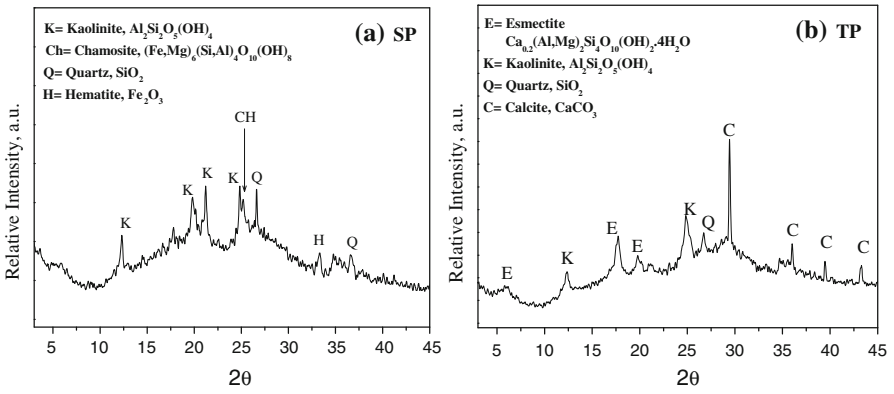

Fig. 3 XRD patterns for samples (**a**) SP and (**b**) ST after calcium carbonate has been dissolved

The PA signal amplitude as a function of time for typical powder samples are shown in Fig. 4b. For SP and TP powdered pellets, it can be observed that the signal is similar to the solid rock ones (Fig. 4a); however, the time interval of decay is shorter than in this last case. This result could be expected since SP and TP samples are compacted powders, with high porosity.

In order to understand our experimental data an effective model was applied, considering that the sample experiences increased wetting as a function of time. Let k_w and k_s be the thermal conductivities of water and stone, respectively; then the effective thermal conductivity k_{eff} can be parameterized in the following form [32],

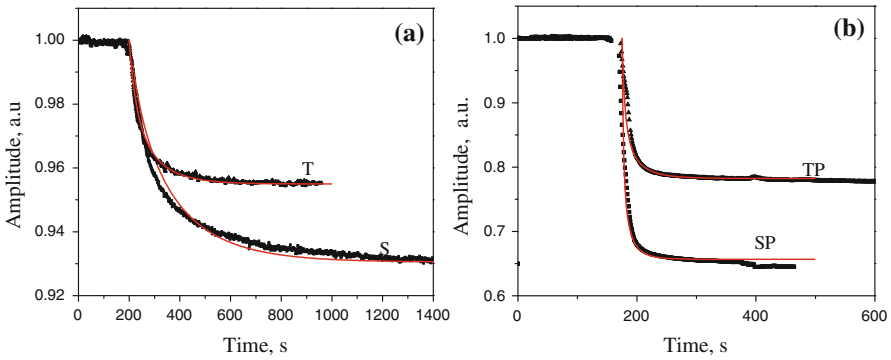

Fig. 4 (**a**) PA signal amplitude as a function of time for S and T samples, during the diffusion process of water in the stone and (**b**) PA signal amplitude as a function of time for SP and TP samples, during the diffusion process of water in the powdered stone

$$k_{\text{eff}} = k_{\text{w}}(1-\phi) + k_{\text{s}}\phi, \tag{3}$$

where the water fraction is $\phi = \frac{V_{\text{w}}}{V_{\text{w}}+V_{\text{s}}} = \frac{m_{\text{w}}}{m_{\text{w}}+um_{\text{s}}}$, with $V_{\text{w}}(m_{\text{w}})$ the volume (mass) of the water that enters into the stone sample with volume (mass) V_{s} (m_{s}) and $u = \frac{\rho_{\text{w}}}{\rho_{\text{s}}}$ where $\rho_{\text{w}} = m_{\text{w}}/V_{\text{w}}$ and $\rho_{\text{s}} = m_{\text{s}}/V_{\text{s}}$ are the densities of the water and stone, respectively. Taking into account that both layers have the same cross section, the effective heat capacity for the system is

$$(\rho c)_{\text{eff}} = (\rho c)_{\text{s}}(1-\phi) + (\rho c)_{\text{w}}\phi, \tag{4}$$

where $(\rho c)_{\text{s}}$ and $(\rho c)_{\text{w}}$ are the volumetric heat capacities of the stone and water, respectively.

From Eqs. 3 and 4, the effective thermal effusivity is obtained;

$$\varepsilon_{\text{eff}} = \sqrt{k_{\text{eff}}(\rho c)_{\text{eff}}} = \sqrt{k_{\text{s}}(\rho c)_{\text{s}}}\left\{\left[(1-\phi)+\frac{k_{\text{w}}}{k_{\text{s}}}\phi\right]\left[(1-\phi)+\frac{(\rho c)_{\text{w}}}{(\rho c)_{\text{s}}}\phi\right]\right\}^{1/2}. \tag{5}$$

Solving the mass diffusion equation with the boundary conditions of a constant water concentration at the top of the rock sample and a null mass flux at the bottom of the sample, due to the presence of the aluminum substrate, it can be shown that the time mass evolution in third order is given by [33]

$$m_{\text{w}} = m_{\text{f}} - \frac{8m_{\text{f}}}{\pi^2}\left\{e^{-\frac{D\pi^2 t}{4l^2}} + \frac{1}{9}e^{-\frac{3D\pi^2 t}{4l^2}} + \frac{1}{25}e^{-\frac{5D\pi^2 t}{4l^2}}\right\}, \tag{6}$$

where D is the water diffusion coefficient, m_{f} is the final mass of water that goes inside the sample at the end of the diffusion process, l is the thickness of the sample, and t is the time.

In Fig. 4, the continuous lines represent the fits of the experimental data using Eq. 6 and the obtained fitted parameters are presented in Table 1. It can be observed that the

Table 1 Diffusion coefficient for limestone samples

Sample	D ($cm^2 \cdot s^{-1}$)
S	$(20 \pm 2) \times 10^{-6}$
T	$(330 \pm 32) \times 10^{-6}$
SP	$(500 \pm 52) \times 10^{-6}$
TP	$(300 \pm 29) \times 10^{-6}$

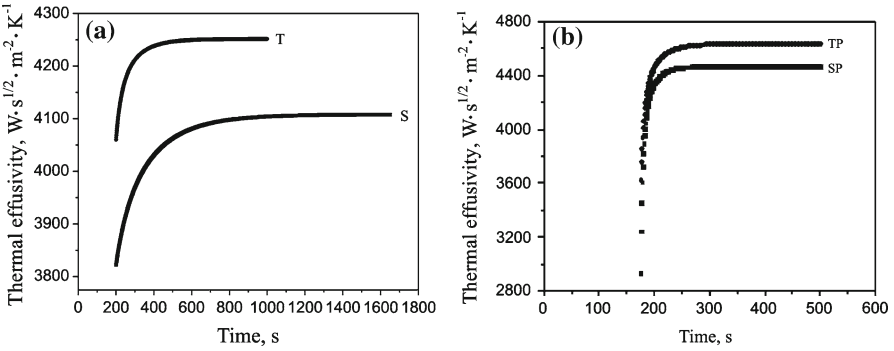

Fig. 5 (**a**) Time evolution of thermal effusivity for S and T samples during the permeation process and (**b**) time evolution of thermal effusivity for SP and TP powder during the permeation process

water diffusion coefficient is very low for the S sample, being 15 times smaller than that in the case of T and TP. However, for the SP sample, the water diffusion coefficient is 25 times larger than the value for S. These values have a direct relationship with the porosity of the samples. In fact, the value of the coefficient for T stones is similar for the solid and powdered samples. This indicates that compacting of the powdered T stone occurs in such a way that the porosity is similar to the solid ones. This can be interpreted as a result of a good compacting process. In contrast, the compacting process of the S rocks resulted in samples with very high water permeation, higher than any other case. Also, this indicates that the compaction process results in many porosity and water permeation channels in S rocks. These are very important results that indicate that the use of the solid material or the pellet has similar results for the water permeation for T rocks and quite different for S rocks, and consequently, they must be considered for building purposes and for applications in soil physics.

Our experimental methodology also allows acquisition of the temporal evolution of the effective thermal effusivity (Fig. 5) using Eq. 5. It can be observed that the effective thermal effusivity increases, after the water drop is placed over the samples. The increment in the thermal effusivity as a function of time is less than 10 % for both cases. However, the coquine limestone (T) shows a faster wetting effect during the first 200 s since it has a higher porosity matrix, compared with the consolidated limestone (S) that takes 450 s.

In contrast, the thermal effusivity for the powdered-pellet samples (Fig. 5b), SP and TP, increases very steeply in a very short period of time of about 25 s. It shows a similar behavior for the two types of samples, exhibiting an increase higher than 30 %.

4 Conclusions

The conventional PA technique was used to monitor in real time the permeation process of water in two kinds of stone (consolidated and coquine limestone) and powdered-pellet stones. Using a simple effective model, the permeation process can be understood as a progressive increment in the sample thermal effusivity. Using this approach, the water diffusion coefficient was determined. It can be demonstrated that the water diffusion process is very low for S samples, being similar for T and TP. However for SP samples, the water diffusion coefficient is 25 times larger than the value for the S sample. These values have a direct relationship with the porosity of the samples, indicating that the compaction process is much better in the T samples than in the S samples. These results are important since they indicate that the use of the solid material or the compacted powder of T rocks has similar results for the water permeation and quite different for S rocks, and consequently, they must be considered for building purposes and for applications in soil physics.

Acknowledgments This study was partially supported by the CONACYT 49275-F (24214), Multidisciplinary-Cinvestav 2009, FOMIX No. 108160 and 108528 projects. The authors want to express their acknowledgment to M.S. J. Bante, M.S. D. Aguilar, and M.S. Dora H. Quintanilla, for their valuable help in the PA cell and electronic construction, characterization, and SEM images-EDAX, respectively.

References

1. N. Cueto, D. Benavente, J. Martínez-Martínez, M.A. García-del-Cura, Eng. Geol. **107**, 1 (2009)
2. D. Benavente, J. Martínez-Martínez, N. Cueto, M.A. García-del-Cura, Eng. Geol. **94**, 215 (2007)
3. H. Ni, H. Behrens, Y. Zhang, Geochim. Cosmochim. Acta **73**, 3642 (2009)
4. M. Raimondo, M. Dondi, D. Gardini, G. Guarini, F. Mazzanti, Constr. Build. Mater. **23**, 2623 (2009)
5. B.O. Ortega-Morales, C.C. Gaylarde, G.E. Englert, P.M. Gaylarde, Int. Biodeter. Biodeg. **58**, 119 (2006)
6. H. Sakuma, K. Kawamura, Geochim. Cosmochim. Acta **73**, 4100 (2009)
7. C. Liu, J.M. Zachara, W. Yantasee, P.D. Majors, J.P. McKinley, Water. Resour. Res. **42**, W12420 (2006)
8. D. Benavente, G. Cultrone, M. Gómez-Heras, Eur. J. Miner. **20**, 673 (2008)
9. B.O. Ortega-Morales, C.C. Gaylarde, G.E. Englert, P.M. Gaylarde, J. Geomicrobiol. **22**, 261 (2005)
10. J. Šperl, J. Trčková, Acta Geodyn. Geomater. **5**, 41 (2008)
11. H. Sudo, T. Tanaka, T. Kobayashi, T. Kondo, T. Takahashi, M. Miyamoto, M. Amagai, Explor. Geophys. **35**, 56 (2005)
12. L. Espinosa, M. Ceron, Y.A. Sulub, Int. J. Rocks Mech. Miner. Sci. Geomech. **35**, 410 (1966)
13. R. Bernal, F.J. Espinoza Beltran, R. Ramirez Bon, S. Sekerj-Zenkovitch, Sup. Vacio **7**, 59 (1997)
14. D. Almond. P. Patel, in *Photothermal Science and Techniques, Physics and its Aplications*, ed. by E.R. Dobbs, S.B. Palmer (Chapman and Hall, London, 1996)
15. A. Mandelis, *Non-Destructive Evaluation: Progress in Photothermal and Photoacoustic Science and Technology*, vol. 2 (PTR Prentice Hall, Englewood Cliffs, NJ, 1993)
16. H. Vargas, L.C.M. Miranda, Phys. Rep. **161**, 43 (1988)
17. S.E. Bialkowski, *Photothermal Spectroscopy Methods for Chemical Analysis* (Wiley, New York, 1996)
18. D. Acosta-Avalos, J.J. Alvarado-Gil, H. Vargas, J. Frías-Hernández, V. Olalde-Portugal, L.C.M. Miranda, Plant Sci. **119**, 183 (1996)
19. A. Frandas, D. Paris, C. Bissieux, M. Chirtoc, J.S. Antoniow, M. Egée, Appl. Phys. B **71**, 69 (2000)
20. A. Landa, J.J. Alvarado-Gil, J. Gutiérrez-Juárez, M. Vargas-Luna, Rev. Sci. Instrum. **74**, 377 (2003)
21. P. Martínez-Torres, J.J. Alvarado-Gil, Int. J. Thermophys. **28**, 996 (2007)
22. D.Y. Fan, R.F. Gao, J. Integr. Plant Biol. **47**, 567 (2005)
23. M.Z. Silva, P. Forge, F. Lepoutre, J. Phys.: Condens. Matter **7**, 9401 (1995)
24. F. Taillade, M.Z. Silva, F. Lepoutre, M. Lecollinet, P. Pinot, Metrologia **38**, 107 (2001)

25. J.H. Rohling, J. Shen, C. Wang, J. Zhou, C.E. Gu, Appl. Phys. B. **87**, 355 (2007)
26. J.A.P. Lima, M.S.O. Massunaga, H. Vargas, L.C.M. Miranda, Anal. Chem. **72**, 114 (2004)
27. L.C.M. Miranda, N. Cella, Phys. Rev. B **47**, 3896 (1993)
28. P. Martínez-Torres, J.J. Alvarado-Gil, Eur. Phys. J. Special Topics **153**, 65 (2008)
29. C.A.S. Lima, L.C.M. Miranda, H. Vargas, Instrum. Sci. Technol. **34**, 191 (2006)
30. M. Vargas-Luna, G. Gutiérrez-Juárez, J.M. Rodríguez-Vizcaíno, J.B. Varela-Nájera, J.M. Rodríguez-Palencia, J. Bernal-Alvarado, M. Sosa, J.J. Alvarado-Gil, J. Phys. D: Appl. Phys. **35**, 1532 (2002)
31. A. Rosencwaig, A. Gersho, J. Appl. Phys. **47**, 64 (1976)
32. S. Torquato, *Random Heterogeneous Materials* (Springer-Verlag, New York, 2001)
33. J. Crank, *The Mathematics of Diffusion* (Clarendon Press, Oxford, 1975)